

Superconducting order parameter of the nodal-line semimetal NaAlSi

Lukas Muechler,¹ Zurab Guguchia,² Jean-Christophe Orain,² Jürgen Nuss,³ Leslie M. Schoop,⁴ Ronny Thomale,⁵ and Fabian O. von Rohr^{6,7}

¹*Center for Computational Quantum Physics, The Flatiron Institute, New York, New York 10010, USA*

²*Laboratory for Muon Spin Spectroscopy, Paul Scherrer Institute, CH-5232 Villigen PSI, Switzerland*

³*Max Planck Institute for Solid State Research, Heisenbergstr. 1, 70569 Stuttgart, Germany*

⁴*Department of Chemistry, Princeton University, 08544 Princeton, NJ, USA*

⁵*Institute for Theoretical Physics and Astrophysics, Julius-Maximilians University of Würzburg, 97074 Würzburg, Germany*

⁶*Department of Chemistry University of Zurich, CH-8057 Zürich, Switzerland*

⁷*Department of Physics, University of Zurich, CH-8057 Zürich, Switzerland*

Abstract. Nodal-line semimetals are topologically non-trivial states of matter featuring band crossings along a closed curve, i.e. nodal-line, in momentum space. Through a detailed analysis of the electronic structure, we show for the first time that the normal state of the superconductor NaAlSi, with a critical temperature of $T_c \approx 7$ K, is a nodal-line semimetal, where the complex nodal-line structure is protected by non-symmorphic mirror crystal symmetries. We further report on muon spin rotation experiments revealing that the superconductivity in NaAlSi is truly of bulk nature, featuring a fully gapped Fermi-surface. The temperature-dependent magnetic penetration depth can be well described by a two-gap model consisting of two *s*-wave symmetric gaps with $\Delta_1 = 0.6(2)$ meV and $\Delta_2 = 1.39(1)$ meV. The zero-field muon experiment indicates that time-reversal symmetry is preserved in the superconducting state. Our observations suggest that notwithstanding its topologically non-trivial band structure, NaAlSi may be suitably interpreted as a conventional London superconductor, while more exotic superconducting gap symmetries cannot be excluded. The intertwining of topological electronic states and superconductivity renders NaAlSi a prototypical platform to search for unprecedented topological quantum phases.

Keywords: Nodal-line semimetals, topological semimetal, superconductor, μ SR

I. INTRODUCTION

In the course of the advent of topological insulators, several classes of non-trivial topological semimetals have been proposed and experimentally sought after: Weyl semimetals, Dirac semimetals, and nodal-line semimetals¹⁻⁵. In their essence, all these types of topological matter arise from band inversion, often along with non-symmorphic symmetries. As opposed to insulators, the topological nature of a semimetal is given by a more intricate version of topological bulk invariants and bulk boundary correspondence. For the most elementary instance, the surface Fermi arcs of a Weyl semimetal are localized away from the Weyl cone projection points at the surface, and derive their localization length scale from the direct gap between the underlying bulk and valence bands at the given surface momentum. For nodal-line semimetals, the surface states feature intriguing structures referred to as drumhead states. Additional complexity can arise if the closed nodal-line takes on more complicated forms in momentum space, which yields structures called nodal knot semimetals. The higher the semimetallic topological complexity the harder it appears to find quantum matter realizations of such states, so classical metamaterial platforms often seem to be the only viable alternative^{6,7}.

In many respects, however, only quantum material realizations of topological semimetals promise a complete unfolding of their rich phenomenology^{8,9}. The interplay of emergent quantum effects such as magnetism, charge-ordering, and superconductivity, together with nontrivial band topology has been identified as a promising platform for the realization of exotic quasi particles, such as e.g. Majorana fermions¹⁰⁻¹³. Recently, several candidates for topological materials with bulk superconductivity have been experimentally realized. Among those are topological insulators, namely $\text{Cu}_x\text{Bi}_2\text{Se}_3$ ¹⁴, or Tl_5Te_3 ¹⁵, Dirac semimetals, namely Cd_3As_2 ¹⁶, Au_2Pb ¹⁷ and 2M-WS_2 ^{18,19}, Weyl semimetals such as MoTe_2 ^{20,21}, and also the nodal-line semimetal PbTaSe_2 ²². Superconducting instabilities of nodal-line semimetals promise to be a particularly interesting class of compounds, as the nodal-lines can induce a Berry phase picked up for a closed path along the Fermi surface and thus constrain possible electronic pairing²³. The only known nodal-line semimetal superconductor, i.e. PbTaSe_2 ²⁴, corresponds to an intercalated derivative of TaSe_2 . This parent compound is a platform for complex charge ordering. Upon intercalation of lead the charge ordering is suppressed and superconductivity is observed at a critical temperature of $T_c \approx 3.8 \text{ K}$ ²⁵.

The ternary compound NaAlSi investigated here crystallizes in the centrosymmetric space group $P4/nmm$ of PbFCl structure-type, as shown in Fig 1(a). This compound is isostructural to the "111" Fe-based superconductors LiFeAs and LiFeP²⁶. NaAlSi has been reported to be a type-II superconductor with a critical temperature of $T_c \approx 7$ K at ambient pressure²⁷, while the isostructural and isoelectronic NaAlGe is not superconducting. NaAlSi and NaAlGe have almost exactly the same band structure except for one missing piece of small Fermi surface. This small Fermi surface is rather unusual, and further obscured by the small but seemingly important interlayer coupling along the crystalline c-axis²⁸. Even though one expects the phonon spectra for these two compounds to be fairly similar, and as such the onset of superconductivity if phonons were responsible for the pairing, the isoelectric cousin NaAlGe does not exhibit any kind of superconductivity down to low temperatures.

H. B. Rhee *et al.* have shown by first-principles electronic structure calculations that NaAlSi is what they refer to as "a naturally self-doped semimetal", with charge-transfer between the covalent bands within the substructure and two-dimensional free-electron-like bands within the Al-Si layers²⁸. This electronic structure results in an unusually small Fermi surface and a very low density of states at the Fermi level. Both characteristics, together with the reasonably high critical temperature of NaAlSi, are contradictory to conventional BCS theory predictions, where the critical temperature T_c depends exponentially on the density of states at the Fermi-level. Given these special electronic features, it was proposed that the superconductivity in this material may not be of phononic origin. Hence, the microscopic origin of superconductivity still remains to be unambiguously identified. It calls for a detailed study of the electronic structure of this nodal-line semimetal, and in particular of how small electronic deviations between NaAlGe and NaAlSi might affect unconventional pairing tendencies from a weak coupling perspective. An unconventional pressure dependence of the superconductivity in NaAlSi has been reported: The critical temperature was found to slightly increase up to a transition temperature of $T_c \approx 9$ K under an external pressure, and to disappear abruptly at a pressure of $p = 4.8$ GPa in the absence of a structural transition²⁹.

Here, we report on detailed band structure calculations, showing that NaAlSi is a nodal-line semimetal for the first time, and on its superconducting order parameter analysis. Our muon spin rotation measurements reveal that the superconductivity in NaAlSi is truly of bulk nature and that the Fermi-surface is fully gapped with an $s + s$ -wave symmetrical gap

Superconducting order parameter of the nodal-line semimetal NaAlSi

in the absence of time-reversal-symmetry breaking. Our observations suggest that superconductivity in this topologically non-trivial material may be explained as a conventional London superconductor. The results, however, do not exclude some more exotic superconducting gap symmetries either, which we will also briefly discuss in this work.

II. METHODS

A. DFT Calculations

The DFT calculations were performed using the *VASP* package³⁰ using the standard pseudopotentials for Na, Si and Al. The experimental geometries were taken from Ref.²⁹. The reducible Brillouin zone was sampled by a $9 \times 9 \times 9$ k-mesh for the self-consistent calculations. A Wannier interpolation using 18 bands was performed by projecting onto an atomic-orbital basis centered at the atomic positions, consisting of Na-3s, Al-3s and 3p as well as Si-3s and 3p orbitals. The nodal-lines were calculated via the package *wanniertools*³¹ based on this Wannier interpolation.

B. Sample Preparation

Blue-metallic, highly crystalline samples of NaAlSi were prepared by solid-state synthesis. In a first step, the elements Na (purity 99.99 %), Al (purity 99.999 %) and Si (purity 99.9999 %) were mixed in a ratio of Na:Al:Si = 3:1:1. The excess of Na is necessary for obtaining phase pure products, it partly acts as a sodium flux. This mixture (2g) was sealed in an argon-filled tantalum tube in order to minimize Na loss during the reaction. The tantalum tube was sealed in a quartz ampule in order to prevent the oxidation of the tantalum reaction vessel. The reaction was carried out at 700 °C for three days (heating rate 50 °C/h). To increase the crystallinity of the product, the sample was slowly cooled (5 °C/h) to 600 °C, held for three days at this temperature, and finally cooled to room temperature (5 °C/h). In a second step, the excess sodium was removed by distillation of the product under a dynamic vacuum at 200 °C for 100 h. The phase purity and crystal structure of the sample was verified by powder and single crystal x-ray diffraction using a D8 Focus diffractometer with Cu $K_{\alpha 1}$ radiation (Bruker AXS GmbH, Karlsruhe, Germany).

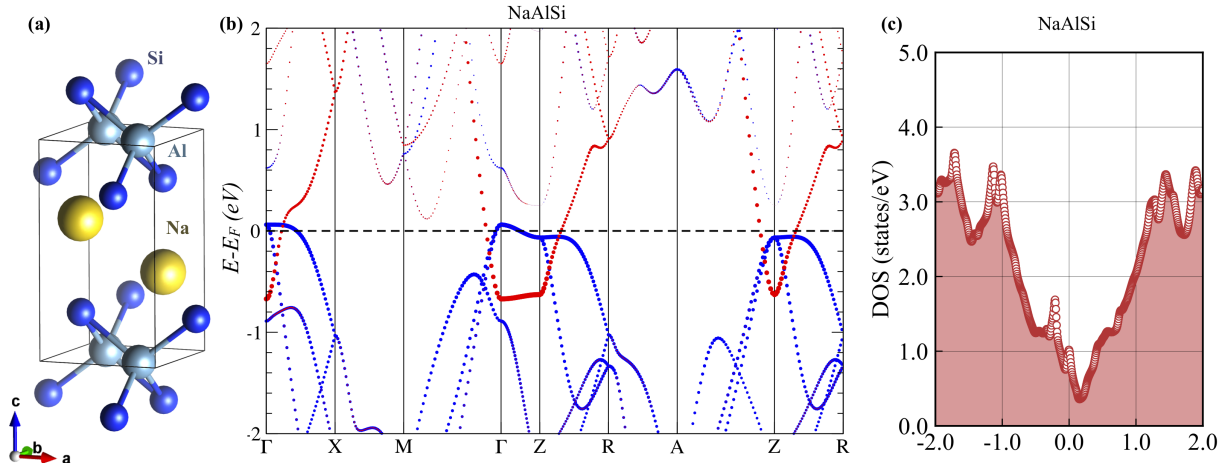


FIG. 1. (a) Crystal structure of NaAlSi (b) Band structure of NaAlSi along high-symmetry points. Blue color indicates contributions from Si- p -orbitals whereas red color indicates Al- p -character. The size of the dots is proportional to the contribution of the orbitals at each k-point. (c) Density of states of bulk NaAlSi between -2 eV to 2 eV from the Fermi-level.

C. μ SR Measurements

Spin-polarized muons (μ^+) are extremely sensitive local magnetic probes that were here used to investigate the field distribution of the vortex state in the type-II superconductor NaAlSi. Transverse field (TF) and zero field (ZF) μ SR experiments were carried down to $T = 250$ mK, well below the superconducting transition temperature of NaAlSi. Pressed pellets of NaAlSi were transferred under inert atmosphere with a portable glovebox into the cryostat. The μ SR spectra have been analyzed using the MUSRFIT software package³².

III. RESULTS AND DISCUSSION

A. Electronic Structure of NaAlSi

Charge balanced materials with 8 valence electrons of the form $X\text{AlSi}$ ($X = \text{Li}, \text{Na}$) are expected to be semiconductors due to a completely filled Si p -shell that is separated by a gap from the empty s -shells of Li^+ and Al^{3+} . While LiAlSi , which crystallizes in the cubic Half-Heusler structure, is indeed a semiconductor with a large direct band gap, NaAlSi shows metallic transport behaviour and becomes superconducting below 7 K. This can be attributed to the fact that NaAlSi does not crystallize in a Half-Heusler structure, but in

the tetragonal spacegroup $P4/nmm$, which consists of edge-sharing AlSi_4 tetrahedra with short Al-Al distances of about 2.9 Å.

The short distance leads to considerable bonding between the Al-atoms in the $x - y$ plane, which is indicated by a dispersive Al- s -band close to the Fermi energy (E_F) with a bandwidth of over 4 eV as shown in Fig 1(b). As expected from the ionic picture discussed above, the band structure close to the Fermi level consists mostly of bands derived from the Si- p -orbitals, which are almost completely filled. However, in contrast to LiAlSi, the large bandwidth with of the Al- s -bands leads to a band inversion between the two sets of bands and results in a metallic band structure with multiple linear band crossings close to E_F in NaAlSi. These band crossings form a complex nodal-line structure, protected by the crystalline symmetries of the space group $P4/nmm$, namely the non-symmorphic mirror symmetry $\bar{M}_z = \{M_z | \frac{1}{2} \frac{1}{2} 0\}$, the mirror M_{xy} , spatial inversion $\{I|000\}$ and the two screw symmetries $\bar{C}_{2x} = \{C_{2x} | \frac{1}{2} 00\}$ and $\bar{C}_{2y} = \{C_{2y} | 0 \frac{1}{2} 0\}$. While nodal-lines and band inversion are a common feature in this space group, the origin of the nodal-lines in NaAlSi is of different origin than those found in e.g. the ZrSiS-family^{33,34} and $\text{FeTe}_{1-x}\text{Se}_x$ ³⁵.

Figure 2 shows the resulting nodal-line structure. It consists of two nodal-lines in the $k_z = 0$ and the $k_z = \pi$ plane, which are interconnected by nodal-lines along the k_z direction. The nodal-line shows dispersion, i.e. the gap closing points do not all occur at one energy, but in a window of about 200 meV around E_F .

B. Temperature dependent magnetic penetration depth

In figure 3(a), we show the transverse-field (TF) μSR -time spectra for NaAlSi, measured in an applied magnetic field of $\mu_0 H = 20$ mT. The spectra above (8 K) and below (0.25 K) the superconducting transition temperature T_c are depicted. In the normal state, the oscillations show a small relaxation due to the random local fields from the nuclear magnetic moments. Below the critical temperature T_c the relaxation rate strongly increases with decreasing temperature due to the presence of a nonuniform local magnetic field distribution as a result of the formation of a flux-line lattice (FLL) in the superconducting state. This is the first reported evidence, in the absence of specific heat measurements, for the bulk nature of the superconductivity in this material.

Magnetism, if present in the samples, may also enhance the muon depolarization rate.

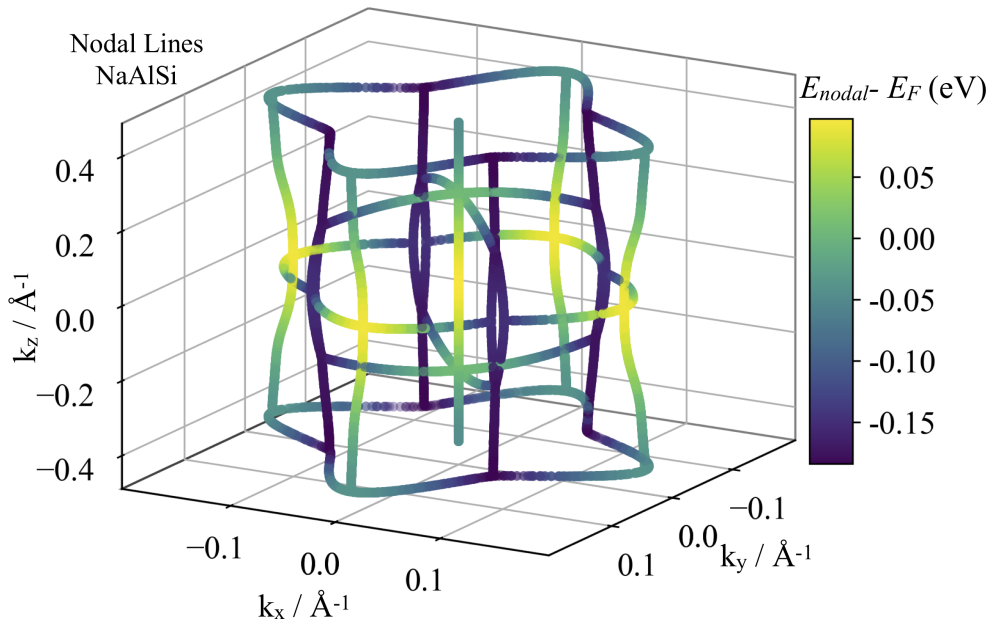


FIG. 2. Nodal-lines derived from the overlap of the highest energy Si- p -band with the Al- s -band. The energy of the crossing point is given relative to E_F .

Therefore, we have carried out ZF- μ SR experiments above and below T_c to search for magnetism (static or fluctuating) in NaAlSi. As shown in figure 3b no sign of either static or fluctuating magnetism could be detected in ZF time spectra down to 0.25 K. The spectra are well described by a weakly damped Kubo-Toyabe depolarization function³⁶, reflecting the field distribution at the muon site created by the nuclear and weak electronic moments. Moreover, no change in ZF- μ SR relaxation rate (see figure 3c) across T_c was observed, pointing to the absence of any spontaneous magnetic fields associated with time-reversal symmetry breaking pairing state in NaAlSi (compare references 37–39).

The temperature dependence of the muon spin depolarization rate σ_{sc} , which is proportional to the second moment of the field distribution (see Method section), of NaAlSi in the superconducting state is shown in figure 3d. Below T_c the relaxation rate σ_{sc} starts to increase from zero with decreasing temperature due to the formation of the FLL. Interestingly, the form of the temperature dependence of σ_{sc} , which reflects the topology of the superconducting gap, shows the saturation upon lowering the temperature below approximately 2 K. We show in the following how these behaviours indicate the presence of the two isotropic s -wave gaps on the Fermi surface of NaAlSi.

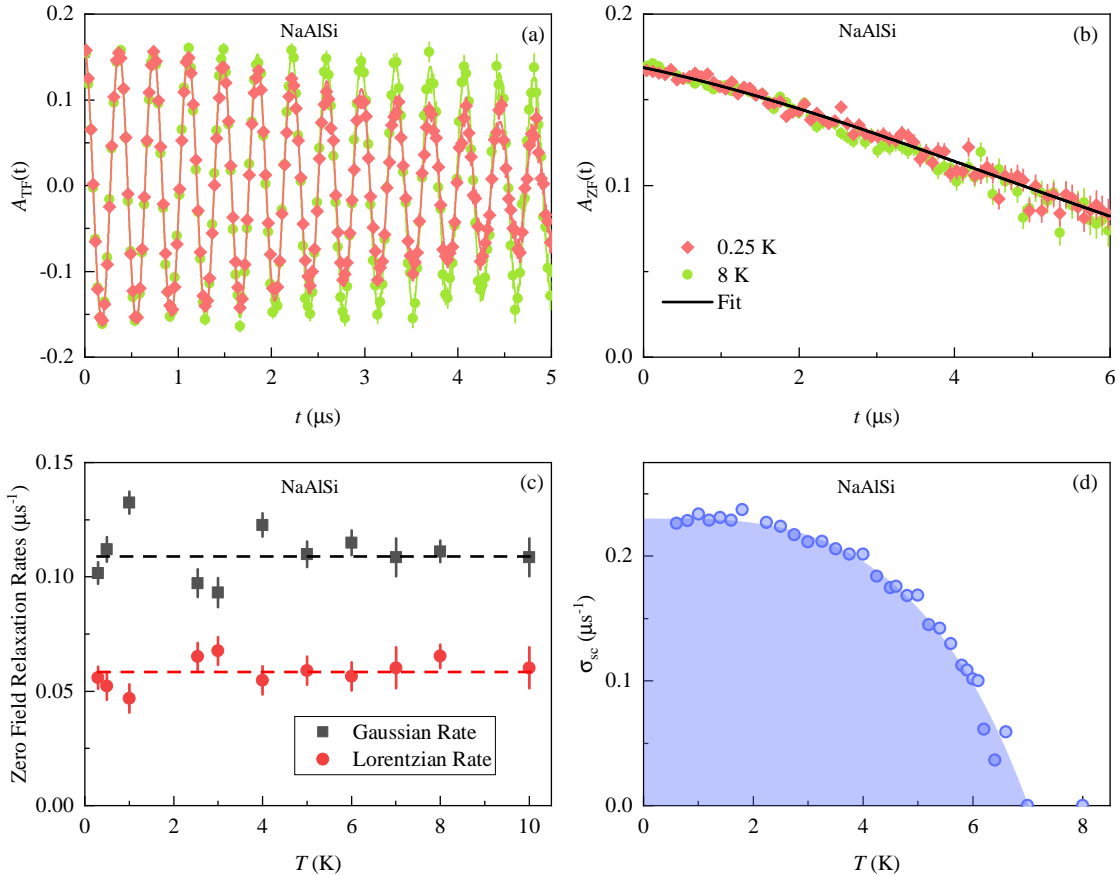


FIG. 3. (a) The transverse-field μ SR time spectra for NaAlSi, obtained above and below T_c (after field cooling the sample from above T_c). The solid lines in represent fits to the data. (b) Zero-field μ SR time spectra for NaAlSi recorded above and below T_c . The line represents the fit to the data of the combination of Lorentzian and Gaussian Kubo-Toyabe depolarization function³⁶. (c) The temperature dependence of the ZF Gaussian and Lorentzian depolarization rates. (d) The temperature dependence of the superconducting muon spin depolarization rate σ_{sc} for NaAlSi, measured in an applied magnetic field of $\mu_0 H = 20$ mT.

C. Probing the nonuniform field distribution in the vortex state

In order to investigate the symmetry of the superconducting gap, we note that $\lambda(T)$ is related to the relaxation rate $\sigma_{sc}(T)$ by the equation⁴⁰

$$\frac{\sigma_{sc}(T)}{\gamma_\mu} = 0.06091 \frac{\Phi_0}{\lambda^2(T)}, \quad (1)$$

where γ_μ is the gyromagnetic ratio of the muon, and Φ_0 is the magnetic-flux quantum. Thus, the flat T -dependence of σ_{sc} observed for low temperatures (see figure 3(d))

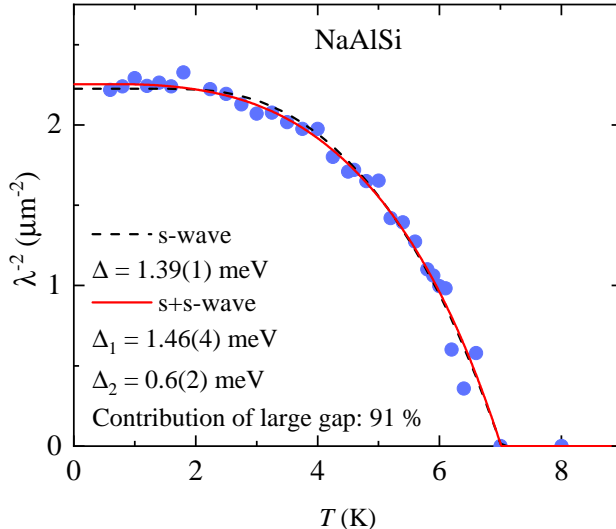


FIG. 4. The temperature dependence of λ^{-2} for NaAlSi. The solid line corresponds to a two-gap ($s+s$)-wave model and the dashed line represents a fit using a single gap s -wave model.

is consistent with a nodeless, fully-gapped superconductor, in which $\lambda^{-2}(T)$ reaches its zero-temperature value exponentially.

To proceed with a quantitative analysis, we consider the local (London) approximation ($\lambda \gg \xi$, where ξ is the coherence length) and employ the empirical α -model. The model, widely used in previous investigations of the penetration depth of multi-band superconductors^{41–45} assumes that the gaps occurring in different bands, besides a common T_c , are independent of each other. The superfluid density is calculated for each component separately⁴⁶ and added together with a weighting factor. For our purposes, a two-band model suffices, yielding

$$\frac{\lambda^{-2}(T)}{\lambda^{-2}(0)} = \omega_1 \frac{\lambda^{-2}(T, \Delta_{0,1})}{\lambda^{-2}(0, \Delta_{0,1})} + \omega_2 \frac{\lambda^{-2}(T, \Delta_{0,2})}{\lambda^{-2}(0, \Delta_{0,2})}, \quad (2)$$

where $\lambda(0)$ is the penetration depth at zero temperature, $\Delta_{0,i}$ is the value of the i -th superconducting gap ($i = 1, 2$) at $T = 0$ K, and ω_i is the weighting factor which measures their relative contributions to λ^{-2} (i.e. $\omega_1 + \omega_2 = 1$).

The results of this analysis are presented in figure 4, where the temperature dependence of λ^{-2} for NaAlSi is plotted. We consider two different possibilities for the gap functions: either a constant gap, $\Delta_{0,i} = \Delta_i$, or an angle-dependent gap of the form $\Delta_{0,i} = \Delta_i \cos 2\varphi$, where φ is the polar angle around the Fermi surface. The dashed and the solid lines represent a fit to the data using an s -wave and an $s + s$ -wave model, respectively. The two gap $s +$

s -wave scenario with a small gap $\Delta_1 \simeq 0.6(2)$ meV and a large gap $\Delta_2 \simeq 1.39(1)$ meV (with the weighting factor of $\omega_2 = 0.91$), describes the experimental data slightly better than the single gap s -wave model, while the relative weight of the small gap is only approximately 10 %. This result might also correspond to a single anisotropic gap with s -wave symmetry, this analysis is insensitive to these different scenarios (compare, e.g., references 21, 43–45).

Even though a phonon-driven mechanism for superconductivity appears likely, and from there a conventional s -wave type order parameter, the experimental evidence reported by us for NaAlSi raises the question of what kind of superconducting order parameter symmetries can in principle be imagined for such a compound. The reported bulk gap excludes nodes in the superconducting phase, and the absence of a zero field signal in μ SR strongly implies preserved time reversal symmetry in the superconductor. The given space group, combined with the co-dimension $p = 2$ of the Fermi surface in the normal state, does not exclude alternative pairings to trivial s -wave. Naively, the point group D_{4h} of NaAlSi possesses three irreducible representations, A_{1g} , B_{1g} and B_{2g} , that are consistent with singlet pairing in the case of vanishing spin-orbit coupling. Since all evidence disfavors line nodes in the superconducting phase and time-reversal symmetry is kept, A_{1g} is the likeliest of a possible two-dimensional irreducible representations. In terms of unconventional pairing, the options are therefore reduced to very exotic superconducting symmetries, such as e.g. helical superconductors, or (slightly more realistically) a relative sign change between the two s -wave sheets. The experiments at hand cannot alone distinguish between sign changing s^{+-} , hence topological, and s^{++} trivial pairing states. Generally, s^{++} can be considered as more likely. However, the high sensitivity of the superconducting state in NaAlSi to disorder, might suggest that a s^{+-} might be realized in this material. Further surface probes such as, e.g., the Kerr effect or phase sensitive measurements, however, would be needed to reach conclusive statements on such questions.

IV. CONCLUSION

In summary, we have reported on a detailed analysis of the electronic structure of the compound NaAlSi. We here describe for the first time that the superconductor NaAlSi has a topological non-trivial nodal-line band structure. Its complex nodal-line structure is thereby

protected by the symmetry of its crystal structure, in particular by the non-symmorphic mirror symmetries of space group $P4/nmm$. We have characterized the microscopic superconducting properties of NaAlSi by a series of μ SR experiments. The TF μ SR experiments reveal for the first time unambiguously that the superconductivity in NaAlSi is of bulk nature. The measured temperature-dependant magnetic penetration depth λ corresponds to a fully-gapped Fermi-surface. In our analysis an $s + s$ -wave symmetrical gap with $\Delta_1 = 0.6(2)$ meV and $\Delta_2 = 1.39(1)$ meV was sufficient to explain the observed behavior. The ZF μ SR experiments above and below the critical temperature indicated the preservation of time reversal symmetry.

Our results indicate that superconductivity in this topologically non-trivial material may be explained as a conventional London superconductor. These results, however, also do not exclude some more exotic superconducting gap symmetries, such as e.g. a s^{+-} symmetric gap. It may be speculated, whether the observed disappearance of superconductivity under pressure or the absence of superconductivity in isoelectronic and isostructural NaAlGe could be tied to the change in topological class in this material. Further theoretical as well as experimental (especially measurements of the bandstructure and thermodynamic measurements of the superconducting properties) work are crucial for understanding the interplay of superconductivity and topology in this material. We expect the results at hand to generally motivate significant additional studies into materials that couple topology to emergent quantum effects.

V. ACKNOWLEDGEMENT

We thank Sabine Prill-Diemer (Max Planck Institute, Stuttgart) for help with the synthesis, Yan Sun for help related to the creation of the Wannier functions, as well as Mark H. Fischer for helpful discussion. The μ SR experiments were carried out at the Swiss Muon Source (S μ S) Paul Scherrer Insitute, Villigen, Switzerland. This work was supported by the Swiss National Science Foundation under Grant No. PZ00P2_174015 and the Ernst Göhner Fellowship 2019 awarded by the "Fond zur Förderung des akademischen Nachwuchs" (FAN). The Flatiron Institute is a division of the Simons Foundation. The work in Würzburg is funded by the Deutsche Forschungsgemeinschaft (DFG, German Research Foundation) through Project-ID 258499086 - SFB 1170 and through the Würzburg-Dresden Cluster of

Excellence on Complexity and Topology in Quantum Matter – *ct.qmat* Project-ID 39085490 - EXC 2147. Work at Princeton was supported by NSF through the Princeton Center for Complex Materials, a Materials Research Science and Engineering Center DMR-1420541. **Note:** This manuscript was submitted to *APL Materials* on August 12, 2019.

REFERENCES

- ¹H. Weng, C. Fang, Z. Fang, B. A. Bernevig, and X. Dai, “Weyl Semimetal Phase in Noncentrosymmetric Transition-Metal Monophosphides,” *Phys. Rev. X* **5**, 011029 (2015).
- ²S.-Y. Xu, I. Belopolski, N. Alidoust, M. Neupane, G. Bian, C. Zhang, R. Sankar, G. Chang, Z. Yuan, C.-C. Lee, *et al.*, “Discovery of a Weyl fermion semimetal and topological Fermi arcs,” *Science* **349**, 613–617 (2015).
- ³B. Bradlyn, J. Cano, Z. Wang, M. G. Vergniory, C. Felser, R. J. Cava, and B. A. Bernevig, “Beyond dirac and weyl fermions: Unconventional quasiparticles in conventional crystals,” *Science* **353** (2016).
- ⁴A. A. Burkov, M. D. Hook, and L. Balents, “Topological nodal semimetals,” *Phys. Rev. B* **84**, 235126 (2011).
- ⁵T. Bzdušek, Q. Wu, A. Rüegg, M. Sigrist, and A. A. Soluyanov, “Nodal-chain metals,” *Nature* **538**, 75 (2016).
- ⁶C.-H. Lee, T. Hofmann, T. Helbig, Y. Liu, X. Zhang, M. Greiter, and R. Thomale, “Imaging nodal knots in momentum space through topoelectrical circuits,” arXiv preprint arXiv:1904.10183 (2019).
- ⁷Z. Yang, C.-K. Chiu, C. Fang, and J. Hu, “Evolution of nodal lines and knot transitions in topological semimetals,” arXiv preprint arXiv:1905.00210 (2019).
- ⁸S. Sur and R. Nandkishore, “Instabilities of Weyl loop semimetals,” *New Journal of Physics* **18**, 115006 (2016).
- ⁹M. Laubach, C. Platt, R. Thomale, T. Neupert, and S. Rachel, “Density wave instabilities and surface state evolution in interacting Weyl semimetals,” *Phys. Rev. B* **94**, 241102 (2016).
- ¹⁰C. Nayak, S. H. Simon, A. Stern, M. Freedman, and S. Das Sarma, “Non-abelian anyons and topological quantum computation,” *Rev. Mod. Phys.* **80**, 1083–1159 (2008).

- ¹¹H. Shapourian, Y. Wang, and S. Ryu, “Topological crystalline superconductivity and second-order topological superconductivity in nodal-loop materials,” *Phys. Rev. B* **97**, 094508 (2018).
- ¹²X.-L. Qi and S.-C. Zhang, “Topological insulators and superconductors,” *Rev. Mod. Phys.* **83**, 1057–1110 (2011).
- ¹³P. Hosur, P. Ghaemi, R. S. K. Mong, and A. Vishwanath, “Majorana modes at the ends of superconductor vortices in doped topological insulators,” *Phys. Rev. Lett.* **107**, 097001 (2011).
- ¹⁴Y. S. Hor, A. J. Williams, J. G. Checkelsky, P. Roushan, J. Seo, Q. Xu, H. W. Zandbergen, A. Yazdani, N. P. Ong, and R. J. Cava, “Superconductivity in $\text{Cu}_x\text{Bi}_2\text{Se}_3$ and its Implications for Pairing in the Undoped Topological Insulator,” *Phys. Rev. Lett.* **104**, 057001 (2010).
- ¹⁵K. E. Arpino, D. C. Wallace, Y. F. Nie, T. Birol, P. D. C. King, S. Chatterjee, M. Uchida, S. M. Koohpayeh, J.-J. Wen, K. Page, C. J. Fennie, K. M. Shen, and T. M. McQueen, “Evidence for Topologically Protected Surface States and a Superconducting Phase in $[\text{Tl}_4](\text{Tl}_{1-x}\text{Sn}_x)\text{Te}_3$ Using Photoemission, Specific Heat, and Magnetization Measurements, and Density Functional Theory,” *Phys. Rev. Lett.* **112**, 017002 (2014).
- ¹⁶A. Aggarwal, L. and Gaurav, G. S. Thakur, Z. Haque, A. K. Ganguli, and G. Sheet, “Unconventional superconductivity at mesoscopic point contacts on the 3D Dirac semimetal Cd_3As_2 ,” *Nature materials* **15**, 32 (2016).
- ¹⁷L. M. Schoop, L. S. Xie, R. Chen, Q. D. Gibson, S. H. Lapidus, I. Kimchi, M. Hirschberger, N. Haldolaarachchige, M. N. Ali, C. A. Belvin, T. Liang, J. B. Neaton, N. P. Ong, A. Vishwanath, and R. J. Cava, “Dirac metal to topological metal transition at a structural phase change in Au_2Pb and prediction of F_2 topology for the superconductor,” *Phys. Rev. B* **91**, 214517 (2015).
- ¹⁸Y. Yuan, J. Pan, X. Wang, Y. Fang, C. Song, L. Wang, K. He, X. Ma, H. Zhang, F. Huang, W. Li, and Q.-K. Xue, “Evidence of anisotropic Majorana bound states in 2M-WS_2 ,” *Nature Physics* (2019).
- ¹⁹Z. Guguchia, D. Gawryluk, M. Brzezinska, S. S. Tsirkin, R. Khasanov, E. Pomjakushina, F. O. von Rohr, J. Verezhak, M. Z. Hasan, T. Neupert, H. Luetkens, and A. Amato, “Nodeless Superconductivity and its Evolution with Pressure in the Layered Dirac Semimetal 2M-WS_2 ,” arXiv preprint arXiv:1903.10612 (2019).

- ²⁰Y. Qi, P. G. Naumov, M. N. Ali, C. R. Rajamathi, W. Schnelle, O. Barkalov, M. Haffand, S.-C. Wu, C. Shekhar, Y. Sun, V. S. M. Schmidt, U. Schwarz, E. Pippel, P. Werner, R. Hillebrand, T. Frster, E. Kampert, S. Parkin, R. J. Cava, C. Felser, B. Yan, and S. A. Medvedev, “Superconductivity in weyl semimetal candidate MoTe₂,” *Nature Communications* **7**, 11038 (2016).
- ²¹Z. Guguchia, F. von Rohr, Z. Shermadini, A. T. Lee, S. Banerjee, A. R. Wieteska, C. A. Marianetti, B. A. Frandsen, H. Luetkens, Z. Gong, S. C. Cheung, C. Baines, A. Shengelaya, G. Taniashvili, A. N. Pasupathy, E. Morenzoni, S. J. L. Billinge, A. Amato, R. J. Cava, R. Khasanov, and Y. J. Uemura, “Signatures of the topological s^{+-} superconducting order parameter in the type-II Weyl semimetal T_d-MoTe₂,” *Nature Communications* **8**, 1082 (2017).
- ²²G. Bian, T.-R. Chang, R. Sankar, S.-Y. Xu, H. Zheng, T. Neupert, C.-K. Chiu, S.-M. Huang, G. Chang, I. Belopolski, D. S. Sanchez, M. Neupane, N. Alidoust, C. Liu, B. Wang, C.-C. Lee, H.-T. Jeng, C. Zhang, Z. Yuan, S. Jia, A. Bansil, F. Chou, H. Lin, and M. Z. Hasan, “Topological nodal-line fermions in spin-orbit metal PbTaSe₂,” *Nature Communications* **7**, 10556 (2016).
- ²³C. Fang, H. Weng, X. Dai, and Z. Fang, “Topological nodal line semimetals,” *Chin. Phys. B* **25**, 117106 (2016).
- ²⁴S.-Y. Guan, P.-J. Chen, M.-W. Chu, R. Sankar, F. C., H.-T. Jeng, C.-S. Chang, and T.-M. Chuang, “Superconducting topological surface states in the noncentrosymmetric bulk superconductor PbTaSe₂,” *Science Advances* **2** (2016), 10.1126/sciadv.1600894.
- ²⁵M. N. Ali, Q. D. Gibson, T. Klimczuk, and R. J. Cava, “Noncentrosymmetric superconductor with a bulk three-dimensional Dirac cone gapped by strong spin-orbit coupling,” *Phys. Rev. B* **89**, 020505 (2014).
- ²⁶W. Westerhaus and H.-U. Schuster, “Darstellung und Struktur von NaAlSi und NaAlGe,” *Zeitschrift für Naturforschung B* **34**, 352 (1979).
- ²⁷S. Kuroiwa, H. Kawashima, H. Kinoshita, H. Okabe, and J. Akimitsu, “Superconductivity in ternary silicide NaAlSi with layered diamond-like structure,” *Physica C: Superconductivity* **466**, 11 – 15 (2007).
- ²⁸H. B. Rhee, S. Banerjee, E. R. Ylvisaker, and W. E. Pickett, “NaAlSi: Self-doped semimetallic superconductor with free electrons and covalent holes,” *Phys. Rev. B* **81**, 245114 (2010).

- ²⁹L. Schoop, L. MÜchler, J. Schmitt, V. Ksenofontov, S. Medvedev, J. Nuss, F. Casper, M. Jansen, R. J. Cava, and C. Felser, “Effect of pressure on superconductivity in NaAlSi,” *Phys. Rev. B* **86**, 174522 (2012).
- ³⁰G. Kresse and J. Furthmüller, “Efficiency of ab-initio total energy calculations for metals and semiconductors using a plane-wave basis set,” *Comput. Mat. Sci.* **6**, 15–50 (1996).
- ³¹Q. Wu, S. Zhang, H.-F. Song, M. Troyer, and A. A. Soluyanov, “Wanniertools: An open-source software package for novel topological materials,” *Comput. Phys. Commun.* **224**, 405–416 (2018).
- ³²A. Suter and B. Wojek, “MUSRFIT: A Free Platform-Independent Framework for μ SR Data Analysis,” *Physics Procedia* **30**, 69 – 73 (2012).
- ³³L. M. Schoop, M. N. Ali, C. Straßer, A. Topp, A. Varykhalov, D. Marchenko, V. Duppele, S. S. Parkin, B. V. Lotsch, and C. R. Ast, “Dirac cone protected by non-symmorphic symmetry and three-dimensional Dirac line node in ZrSiS,” *Nat. Commun.* **7**, 11696 (2016).
- ³⁴S. Pezzini, M. R. Van Delft, L. M. Schoop, B. V. Lotsch, A. Carrington, M. I. Katsnelson, N. E. Hussey, and S. Wiedmann, “Unconventional mass enhancement around the Dirac nodal loop in ZrSiS,” *Nat. Phys.* **14**, 178 (2018).
- ³⁵P. Zhang, K. Yaji, T. Hashimoto, Y. Ota, T. Kondo, K. Okazaki, Z. Wang, J. Wen, G. Gu, H. Ding, *et al.*, “Observation of topological superconductivity on the surface of an iron-based superconductor,” *Science* **360**, 182–186 (2018).
- ³⁶R. Kubo and T. Toyabe, “Magnetic resonance and relaxation,” North-Holland, Amsterdam **810** (1967).
- ³⁷G. M. Luke, Y. Fudamoto, K. Kojima, M. Larkin, J. Merrin, B. Nachumi, Y. Uemura, Y. Maeno, Z. Mao, Y. Mori, *et al.*, “Time-reversal symmetry-breaking superconductivity in Sr₂RuO₄,” *Nature* **394**, 558 (1998).
- ³⁸A. D. Hillier, J. Quintanilla, and R. Cywinski, “Evidence for time-reversal symmetry breaking in the noncentrosymmetric superconductor LaNiC₂,” *Phys. Rev. Lett.* **102**, 117007 (2009).
- ³⁹P. Biswas, H. Luetkens, T. Neupert, T. Stürzer, C. Baines, G. Pascua, A. Schnyder, M. Fischer, J. Goryo, M. Lees, *et al.*, “Evidence for superconductivity with broken time-reversal symmetry in locally noncentrosymmetric SrPtAs,” *Phys. Rev. B* **87**, 180503 (2013).
- ⁴⁰E. H. Brandt, “Flux distribution and penetration depth measured by muon spin rotation in high- T_c superconductors,” *Phys. Rev. B* **37**, 2349–2352 (1988).

- ⁴¹M. Tinkham, *Introduction to Superconductivity*, Dover Books on Physics Series (Dover Publications, 2004).
- ⁴²A. Carrington and F. Manzano, “Magnetic penetration depth of MgB₂,” *Physica C* **385**, 205–214 (2003).
- ⁴³H. Padamsee, J. Neighbor, and C. Shiffman, “Quasiparticle phenomenology for thermodynamics of strong-coupling superconductors,” *J. Low Temp. Phys.* **12**, 387–411 (1973).
- ⁴⁴C. Niedermayer, C. Bernhard, T. Holden, R. K. Kremer, and K. Ahn, “Muon spin relaxation study of the magnetic penetration depth in MgB₂,” *Phys. Rev. B* **65**, 094512 (2002).
- ⁴⁵F. von Rohr, J.-C. Orain, R. Khasanov, C. Witteveen, Z. Shermadini, A. Nikitin, J. Chang, A. Wieteska, A. Pasupathy, M. Hasan, *et al.*, “Unconventional scaling of the superfluid density with the critical temperature in transition metal dichalcogenides,” arXiv preprint arXiv:1903.05292 (2019).
- ⁴⁶Z. Guguchia, A. Amato, J. Kang, H. Luetkens, P. K. Biswas, G. Prando, F. von Rohr, Z. Bukowski, A. Shengelaya, H. Keller, *et al.*, “Direct evidence for a pressure-induced nodal superconducting gap in the Ba_{0.65}Rb_{0.35}Fe₂As₂ superconductor,” *Nat. Commun.* **6**, 8863 (2015).